Medium Modifications of Heavy-Flavor Jet Angularities in High-Energy Nuclear Collisions

Yao Li[1], Shi-Yong Chen[2], Wei-Xi Kong[1], Sa Wang[3,4*], and Ben-Wei Zhang[1*]

[1]*Key Laboratory of Quark & Lepton Physics (MOE) and Institute of Particle Physics, Central China Normal University, Wuhan 430079, China*
[2]*Huanggang Normal University, Huanggang 438000, China*
[3]*College of Science, China Three Gorges University, Yichang 443002, China*
[4]*Center for Astronomy and Space Sciences and Institute of Modern Physics, China Three Gorges University, Yichang 443002, China*

(Received 10 October 2024; accepted manuscript online 20 December 2024)

We present the first theoretical study on heavy-flavor jet angularities (λ_α^κ) in Pb+Pb collisions at $\sqrt{s_{\rm NN}} = 5.02$ TeV. The initial production of heavy-flavor jets was carried out using the POWHEG+PYTHIA8 prescription. In contrast, the SHELL transport model describes jet evolution in the quark-gluon plasma (QGP). In p+p collisions, we observed narrower angularity distributions for $\rm D^0$-tagged jets than for inclusive jets, consistent with the ALICE preliminary results. We then demonstrate that jet quenching in the QGP slightly widens the angularity distribution of $\rm D^0$-tagged jets in Pb+Pb collisions relative to that in p+p collisions for a jet transverse momentum of $10 < p_{\rm T,\,jet}^{\rm ch} < 20$ GeV/c. In contrast, the angularity distributions of the inclusive and $\rm D^0$-tagged jets become narrower in Pb+Pb collisions relative to p+p at $p_{\rm T,\,jet}^{\rm ch} > 20$ GeV/c because of the strong influence of selection bias. Additionally, by comparing the average angularities $\langle\lambda_\alpha^\kappa\rangle$ of the inclusive, $\rm D^0$-tagged, and $\rm B^0$-tagged jets with varying α and κ, we show that the larger the quark mass, the lower the jet's $\langle\lambda_\alpha^\kappa\rangle$ values are. As a result of the slenderer initial distribution, we predict that compared with inclusive jets, heavy-flavor jets, especially $\rm B^0$-tagged ones, will suffer stronger modifications of $\langle\lambda_\alpha^\kappa\rangle$ in Pb+Pb relative to p+p at $10 < p_{\rm T,\,jet}^{\rm ch} < 20$ GeV/c. For a larger jet radius, a more significant broadening of the jet angularities was predicted because of the enhanced contribution of the wide-angle particles.

DOI: 10.1088/0256-307X/42/1/011201 CSTR: 32039.14.0256-307X.42.1.011201

1. Introduction. One of the most important topics in heavy-ion physics is understanding the properties of deconfined nuclear matter and quark-gluon plasma (QGP) in high-temperature and high-density environments.[1,2] When an energetic parton passes through the QGP created in high-energy nucleus-nucleus collisions, it may strongly interact with the thermally dense medium, resulting in a loss of its energy and broadening of its transverse momentum, referred to as the "jet quenching" effect.[3–23] In particular, heavy quarks (charm and bottom) are powerful hard probes for studying jet quenching effects because they are produced in the early stages of nuclear collisions and conserve their identity throughout medium evolution (see reviews in Refs. [24–27]). By studying the production of heavy-flavor mesons and jets (a spray of collimated hadrons) in high-energy heavy-ion collisions, the transport properties of the QGP can be effectively extracted. Quantum chromodynamics (QCD) can be further tested under extreme conditions.[28–33]

Over the last two decades, experimental physicists have made significant efforts to investigate the behavior of heavy quarks in heavy-ion collisions, including yield suppression,[34–37] collective flow,[38–40] and baryon-to-meson ratio of heavy-flavor hadrons.[41,42] Simultaneously, theorists have conducted extensive and in-depth research on heavy-quark production,[43,44] the cold nuclear matter (CNM) effect,[45,46] mass-dependent energy loss[47–49] and hadronization mechanisms.[50–52] Recently, studies on heavy-flavor jet observables such as yield suppression,[53,54] transverse momentum balance[55,56] and azimuthal correlations[57] have provided additional insights for further understanding of the mass and flavor dependence of energy loss. In particular, with the help of increased statistics and improvements in experimental detection accuracy, the substructures of heavy quark jets, such as the jet radial profile,[58,59] jet fragmentation function[60] and splitting function,[61] has gradually become a hot topic in theoretical and experimental research in recent years. Substructure observables describe a jet's internal energy distribution and splitting configuration,[62–66] providing a unique perspective for exploring the interactions between heavy quarks and QGP.[58,61,67]

The generalized jet angularities, which quantify the transverse momentum ($p_{\rm T}$), and the angular distributions

*Corresponding author. Email: wangsa@ctgu.edu.cn; bwzhang@mail.ccnu.edu.cn
© 2025 Chinese Physical Society and IOP Publishing Ltd. All rights, including for text and data mining, AI training, and similar technologies, are reserved.

of the constituents within the jet form a class of jet substructure observables,[68] which are defined as

$$\lambda_\alpha^\kappa = \sum_{i\in\text{jet}} \left(\frac{p_{\text{T},i}}{p_{\text{T,jet}}^{\text{ch}}}\right)^\kappa \left(\frac{\Delta R_{\text{jet},i}}{R}\right)^\alpha \equiv \sum_{i\in\text{jet}} z_i^\kappa \theta_i^\alpha, \quad (1)$$

where the index i sums over all jet constituents, R is the jet radius, $\Delta R_{\text{jet},i} = \sqrt{(y_{\text{jet}} - y_i)^2 + (\phi_{\text{jet}} - \phi_i)^2}$ is the angular distance between jet constituent i and the jet axis in the speed (y) and azimuthal angle (ϕ) planes. The parameters κ and α control the weights of the momentum fraction and opening angle of the jet constituents. Recently, the ALICE collaboration reported the measurement of D^0-tagged jet angularities in p+p collisions at $\sqrt{s} = 5.02\,\text{TeV}$,[69] which show smaller values compared to inclusive jets in the same kinematic region. Because the angularity quantifies the p_T-weighted angular distribution of particles in jets,[68] the smaller angularity of D^0-tagged jets indicates a more concentrated energy distribution around the jet axis compared with inclusive jets. It is important to reveal the nature of the different substructures of D^0-tagged jets and inclusive jets.[70–74] Compared to previous heavy-flavor jet substructure measurements that focused on either the angular distribution (radial profile) or momentum fractions (fragmentation and splitting functions) of jet constituents, jet angularities allow us to study the interplay between the two as heavy quarks traverse the QGP.[23,68] Therefore, it is of theoretical significance to investigate the heavy-flavor jet angularities in Pb+Pb collisions, which can be tested using future measurements at the LHC.

We present theoretical studies on heavy-flavor jet angularities in p+p and Pb+Pb collisions at $\sqrt{s_{\text{NN}}} = 5.02\,\text{TeV}$. We now discuss the angular differences between the inclusive and D^0-tagged jets. We present the first calculations of heavy-flavor jet angularities for nucleus-nucleus collisions and compare them with those of light-flavor jets. We further test the sensitivities of the jet angularities and their modifications to parameters α and κ.

2. Jet Angularities in p+p Collisions. In this study, we simulated the production of inclusive and heavy-flavor jets using the POWHEG+PYTHIA8 prescription, which matches the next-to-leading-order (NLO) matrix elements with the resumption of the parton shower (PS).[75–77] QCD dijet processes[78] and the CT18NLO parton distribution function (PDF)[79] were used in the simulations. The hadronization of partons in a vacuum was simulated using the Lund string model implemented in PYTHIA8.[77] Charged hadrons reconstruct inclusive jets, whereas D^0-tagged jets are reconstructed by charged hadrons and neutral D^0 mesons, following the ALICE measurements.[69] Charged hadrons in the jets must have $|\eta| < 0.9$. The anti-k_T algorithm implemented in the FastJet package[80] was used with the jet radius parameter $R = 0.4$. The reconstructed D^0-tagged jets must contain at least one D^0 meson with $p_{\text{T,D}^0} > 5\,\text{GeV/c}$. Inclusive jets are selected by requiring the leading particle to satisfy $p_\text{T} > 5.33\,\text{GeV/c}$ and the same cut on the transverse mass $m_\text{T} = \sqrt{p_\text{T}^2 + m_0^2}$ as D^0-tagged jets, where m_0 is the particle mass and is assumed to be zero for the leading particles in the inclusive jets. In Fig. 1, we show the angularity distributions of the D^0-tagged and inclusive jets for four different values of α: 1.0, 1.5, 2.0, and 3.0, in p+p collisions at $\sqrt{s} = 5.02\,\text{TeV}$ compared with the ALICE preliminary data.[69] Reasonably good agreement is observed, and the D^0-tagged (charm-enriched) jets have distinctly narrower angularity distributions than the inclusive jets for small α, where the mass effects can be critical. From the ratios of D^0-tagged to inclusive jets shown in the bottom panels, it can be observed that our calculations provide a good description of the ALICE data for all values of $\lambda_\alpha^{\kappa=1}$, except for a slight overestimation of the ratios near $\lambda_\alpha^{\kappa=1} \sim 0$. As the value of α increases, the shapes of $\lambda_\alpha^{\kappa=1}$ for the D^0-tagged and inclusive jets begin to converge because wide-angle emissions receive more weight with larger α values.

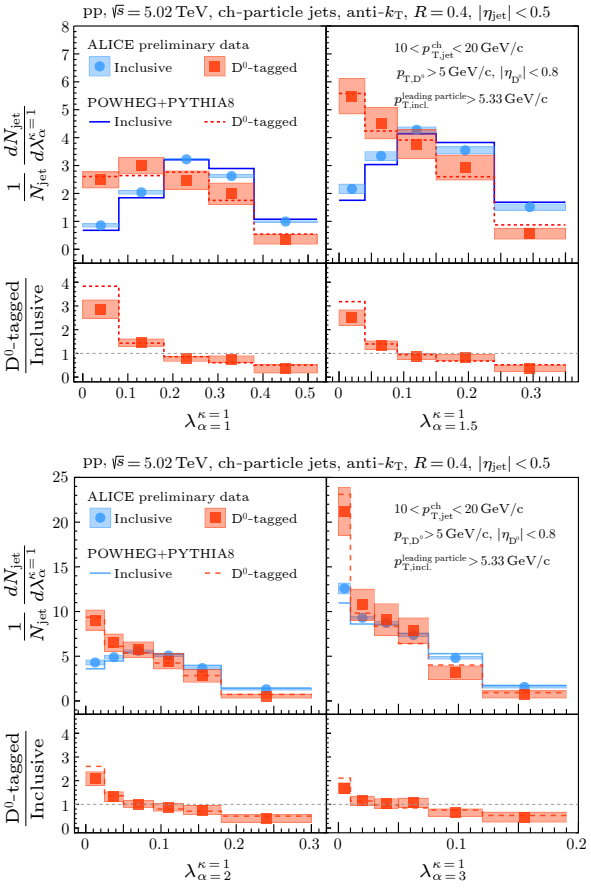

Fig. 1. Normalized angularity distributions of D^0-tagged and inclusive jets for four different values of α: 1.0, 1.5, 2.0, and 3.0 with the fixed $\kappa = 1.0$ in p+p collisions at $\sqrt{s} = 5.02\,\text{TeV}$, compared to the ALICE preliminary data.[69]

We investigated the relationship between jet angularity and flavor to explore the origin of the different angularities for inclusive and D^0-tagged jets. In this study, we employed an infrared-and-collinear-safe jet flavor algorithm, Interleaved Flavor Neutralization (IFN),[81] to identify the jet flavor. Although such flavor identification is not accessible experimentally, conducting such studies using Monte Carlo simulations is still informative. For the production

of heavy quark jets, the pair creation process dominates the low-$p_{\rm T}$ region (above 90% at $10 < p_{\rm T,\,jet}^{\rm ch} < 20\,{\rm GeV/c}$). In contrast, gluon splitting is important at higher $p_{\rm T}$ ($p_{\rm T,\,jet} > 100\,{\rm GeV/c}$).[82,83] Additionally, the inclusive jets were dominated by light quarks and gluon jets. In Fig. 2, we show the angularity distributions of the three types of jets in p+p collisions for $\alpha = 1.0$ (left) and $\alpha = 3.0$ (right). Peaks near $\lambda_\alpha^\kappa \sim 0$ denote jets with only one component. We found that gluon jets have the broadest angularity distributions compared to light quarks and $\rm D^0$-tagged jets. This is because the larger Casimir color factor for gluons leads to more vacuum radiation than for quarks. We also observe that the $\rm D^0$-tagged jets have a narrower angularity distribution than the light-quark jets; such a difference is likely related to the "dead-cone" effect,[84,85] which suppresses small-angle radiation for heavy quarks. As α increases, the differences in the angularities between the $\rm D^0$-tagged and light-quark jets tend to disappear; however, the gluon and light-quark jet angularities remain well separated.

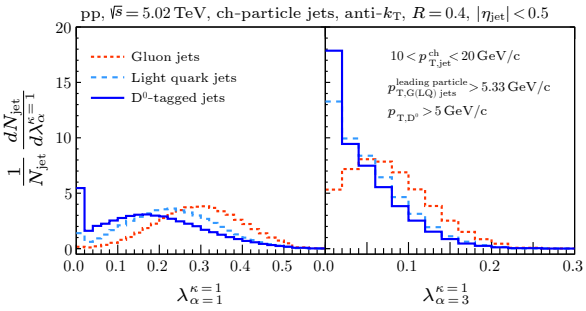

Fig. 2. Normalized angularity distributions of light-quark and gluon jets for $\alpha = 1$ and $\alpha = 3$ with the fixed $\kappa = 1.0$. The angularity distributions of $\rm D^0$-tagged jets are also shown for comparison.

3. Jet Quenching Framework. To simulate the in-medium evolution of both inclusive and heavy-flavor jets, we utilized the Langevin equation (SHELL) model to simulate heavy quark,[55–59] which can simultaneously consider the elastic and inelastic partonic scatterings in the QGP medium. We used the p+p event with a complete vacuum parton shower generated by the POWHEG+PYTHIA8 event generator as the input to the SHELL model. The initial spatial distribution of the partons was sampled using the Monte Carlo-Glauber model.[86] Because the elastic scattering between heavy quarks and thermal partons can be treated as a Brownian motion, the transport of heavy quarks in a hot and dense expanding medium can be well described by the modified Langevin equations as follows:

$$\boldsymbol{x}(t+\Delta t) = \boldsymbol{x}(t) + \frac{\boldsymbol{p}(t)}{E}\Delta t, \tag{2}$$

$$\boldsymbol{p}(t+\Delta t) = \boldsymbol{p}(t) - \eta_{\rm D}\boldsymbol{p}(t)\Delta t + \boldsymbol{\xi}(t)\Delta t - \boldsymbol{p}_{\rm g}, \tag{3}$$

where Δt is the time step of the Monte Carlo simulation, $\boldsymbol{x}(t)$ and $\boldsymbol{p}(t)$ are the position and momentum of the partons at time t, respectively. E is the energy of the parton, and $\eta_{\rm D}$ is the drag coefficient, which controls the energy dissipation strength of heavy quarks in the medium. The stochastic term $\xi(t)$ represents the random kicks on heavy quarks from the thermal partons, which obeys the Gaussian distribution $\langle \xi^i(t)\xi^j(t')\rangle = \kappa\delta^{ij}\delta(t-t')$ with κ being the momentum diffusion coefficient that can be related to $\eta_{\rm D}$ using the fluctuation-dissipation theorem $\kappa = 2\eta_{\rm D}ET$, where T is the temperature of the medium. In the simulations, we set $2\pi T D_{\rm s} = 4.0$, where $D_{\rm s}$ is the spatial diffusion coefficient, which is extracted by a χ^2 fitting to the yield suppression of D mesons measured by CMS[34] and ALICE.[87] On the right-hand side of Eq. (3), the last term, $-p_g$, denotes the momentum shift caused by medium-induced gluon radiation. In our framework, we employed a higher-twist[88–91] formalism to simulate the medium-induced gluon radiation, whose The spectra are as follows:

$$\frac{dN_g}{dx dk_\perp^2 dt} = \frac{2\alpha_{\rm s}C_{\rm s}P(x)\hat{q}}{\pi k_\perp^4}\sin^2\left(\frac{t-t_i}{2\tau_f}\right)\left(\frac{k_\perp^2}{k_\perp^2+x^2M^2}\right)^4, \tag{4}$$

where x and $k_\perp$ denote gluon energy fractions with respect to the parent parton and transverse momentum, respectively. $\alpha_{\rm s}$ is the strong coupling constant and fixed to be 0.3, $C_{\rm s}$ is the quadratic Casimir factor in color representation, $P(x)$ is the QCD splitting function, $t_{\rm i}$ represents the initial moment when the radiation begins, $\tau_{\rm f} = 2Ex(1-x)/(k_\perp^2 + x^2M^2)$ is the formation time of the daughter gluon considering the Landau–Pomeranchuk–Migdal (LPM) effects,[92,93] and $\hat{q} \propto q_0(T/T_0)^3$ is the medium's transport coefficient,[94] where T_0 is the temperature at the center of the medium at 0.6 fm/c. In the simulations, we set $q_0 = 1.2\,{\rm GeV}^2/{\rm fm}$, which was extracted based on the identified hadron production in the A+A collisions, as in our previous work.[95] The last term in Eq. (4) denotes the suppression factor resulting from the "dead-cone" effect, which reduces small angle ($\theta < M_{\rm Q}/E$, $M_{\rm Q}$ being the mass of heavy quarks) gluon radiation.

In the calculation, we utilized the CLVisc hydrodynamic model[96,97] to generate the discrete temperature and velocity of the medium in a space-time grid of the expanding fireball. The local temperature and velocity of the medium through which a parton passes can be obtained by linear interpolation of its time and position according to this grid. When the local temperature reaches the presumptive critical temperature $T_{\rm c} = 0.165\,{\rm GeV}$, the partons fragment into hadrons with the Colorless Hadronization prescription developed by the JETSCAPE collaboration[98] based on the Lund string fragmentation model.[99]

As the energetic parton propagates through the QGP, it loses energy to the medium. It excites a wake correlated with the direction of the parton.[100] After freezing, this wake becomes a soft hadron that is reconstructed as part of the jet, and it is challenging to isolate such a medium response experimentally. As the jet angularities are closely related to the transverse momenta and opening angles of the jet constituents, this medium-response effect must be considered for a fair comparison with the data. We follow the approach of implementing the medium-response effect in the Hybrid Model,[101] which expands the Cooper–Frye formula[102] at the perturbed freeze-out hypersurface, and yields an estimate of the soft hadron spectrum from the

wake:[101]

$$E\frac{d\Delta N}{d^3p} = \frac{1}{32\pi}\frac{m_{\rm T}}{T^5}\cosh(y-y_j)\exp\left[-\frac{m_{\rm T}}{T}\cosh(y-y_j)\right] \times\left\{p_{\rm T}\Delta P_{\rm T}\cos(\phi-\phi_j) + \frac{1}{3}m_{\rm T}\,\Delta M_{\rm T}\,\cosh(y-y_j)\right\}, \quad (5)$$

where $m_{\rm T}$, $p_{\rm T}$, y, and ϕ denote the transverse mass, transverse momentum, rapidity, and azimuthal angle of the emitted wake particles, respectively. y_j and ϕ_j are the rapidity and azimuthal angle of the energetic parton, respectively. T denotes the freeze-out temperature of the hot QCD medium. $\Delta M_{\rm T} = \Delta E/y_j$ and $\Delta P_{\rm T}$ are the transverse mass and momentum transferred from the jet to the medium, respectively, and ΔE is the jet energy loss. The SHELL model has been successfully employed in studies of heavy-flavor jet production in high-energy nuclear collisions, such as yield suppression,[103,104] transverse momentum balance,[55,56] angular correlations,[57,105] and substructure modification.[58–60,106]

4. Numerical Results and Discussions. To validate our model, as introduced in the previous section, we calculated the angularities of the inclusive jets in p+p and 0–10% Pb+Pb collisions at $\sqrt{s_{\rm NN}} = 5.02$ TeV. We compared these results with the ALICE preliminary data[107] as shown in Fig. 3. In line with the ALICE measurements, inclusive jets were reconstructed using charged particles with the anti-$k_{\rm T}$ algorithm for $R = 0.2$ in the kinematic range $40 < p_{\rm T,jet}^{\rm ch} < 60$ GeV/c. Then, the inclusive jets were groomed by a soft drop[108] with the parameters $\beta = 0$ and $z_{\rm cut} = 0.2$. We found that the $\lambda_\alpha^{\kappa=1}$ distributions calculated by POWHEG+PYTHIA8 (p+p) and the SHELL model (Pb+Pb) both provided decent descriptions of the ALICE data for all α. From the ratio of Pb+Pb to pp, we observed an enhancement at small $\lambda_\alpha^{\kappa=1}$ and suppression at large $\lambda_\alpha^{\kappa=1}$ in Pb+Pb collisions relative to p+p, which is consistent with a previous study.[23] The modification pattern of $\lambda_\alpha^{\kappa=1}$ distribution in Pb+Pb collisions can be explained by the "selection bias" effect.[105,109–112] With the steeply falling jet spectrum, the effectively quenched jets may have a lower probability of passing the $p_{\rm T}$ selection threshold in A+A collisions due to the energy loss in the QGP. At the same time, the one with insufficient quenching survives, referred to as the "selection bias". Such a bias can enhance the fraction of narrow jets that experience less energy loss. than wide jets in the selected sample in the A+A collisions compared to that in the p+p collisions. Furthermore, as shown in Fig. 2, quark jets have a narrower angularity distribution than gluon jets in a vacuum. Because gluon jets suffer more energy loss than quark jets in nuclear–nuclear collisions, quark jets have a higher probability of surviving kinematic selection in Pb+Pb collisions. Therefore, an increased fraction of surviving narrow jets can lead to an enhancement in the small $\lambda_\alpha^{\kappa=1}$ region and suppression in the large $\lambda_\alpha^{\kappa=1}$ region in Pb+Pb collisions relative to p+p. More detailed discussions on the influence of selection bias on jet substructure modifications in heavy-ion collisions can be found in Refs. [109–112].

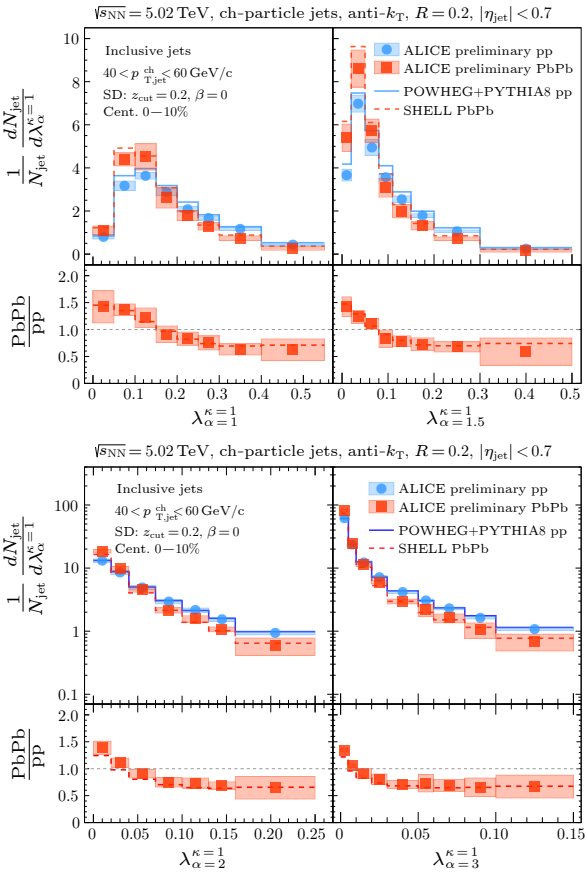

Fig. 3. Normalized angularity distributions of inclusive jets for four different values of α: 1.0, 1.5, 2.0, and 3.0 with the fixed $\kappa = 1.0$ in p+p and 0–10% Pb+Pb collisions at $\sqrt{s_{\rm NN}} = 5.02$ TeV, compared to the ALICE preliminary data.[107] The ratios of PbPb/pp are shown in the lower panel.

Next, we turned to medium modifications of heavy-flavor jet angularities in nucleus-nucleus collisions at the LHC, which have not yet been measured. In Fig. 4, we show the calculations of the jet angularities of the inclusive and $\rm D^0$-tagged jets in p+p and 0–10% Pb+Pb collisions at $\sqrt{s_{\rm NN}} = 5.02$ TeV for three $p_{\rm T,jet}^{\rm ch}$ intervals: $10 < p_{\rm T,jet}^{\rm ch} < 20$ GeV/c, $20 < p_{\rm T,jet}^{\rm ch} < 40$ GeV/c, and $40 < p_{\rm T,jet}^{\rm ch} < 60$ GeV/c, as well as the Pb/pp ratios. In the latter two $p_{\rm T,jet}^{\rm ch}$ intervals, the leading hadron ($\rm D^0$ meson) in the inclusive ($\rm D^0$-tagged) jets must have $p_{\rm T} > 10$ GeV/c and $p_{\rm T} > 15$ GeV/c, respectively. For $p_{\rm T,jet}^{\rm ch} > 20$ GeV/c, the jet angularities become narrower in Pb+Pb collisions compared to those in p+p collisions for both $\rm D^0$-tagged and inclusive jets, which is caused mainly by selection bias. At $10 < p_{\rm T,jet}^{\rm ch} < 20$ GeV/c, we observe that the angularity distributions of the $\rm D^0$-tagged jets become slightly broader in Pb+Pb collisions than in p+p collisions because of the jet quenching effect. Here, a lower $p_{\rm T}$ threshold for jet selection can suppress the influence of selection bias. Because the in-medium radiation of charm quarks reduces the fraction of jets containing only $\rm D^0$ mesons, a remarkable suppression of the $\rm D^0$-tagged jet angularity near $\lambda_{\alpha=1}^{\kappa=1} \sim 0$ can be observed. The modifications of $\lambda_{\alpha=1}^{\kappa=1}$ distributions for inclusive jets are more distinct than those for $\rm D^0$-tagged jets at $p_{\rm T,jet}^{\rm ch} > 20$ GeV/c. This can be explained by the

fact that inclusive jets contain a considerable fraction of gluon jets, which are subject to selection bias to a greater extent than quark jets.[111,112] The effect of the medium response can be studied by comparing the angularity distributions with and without wake particles sampled using Eq. (5). We found a limited impact of the medium response on the jet angularities for a jet radius of $R = 0.2$. In the following discussion, we focus on the medium modification of jet angularities at a lower jet $p_{\rm T}$ ($10 < p_{\rm T,jet}^{\rm ch} < 20\,{\rm GeV/c}$), where the jet quenching effect is pronounced. The influence of selection bias is moderate.

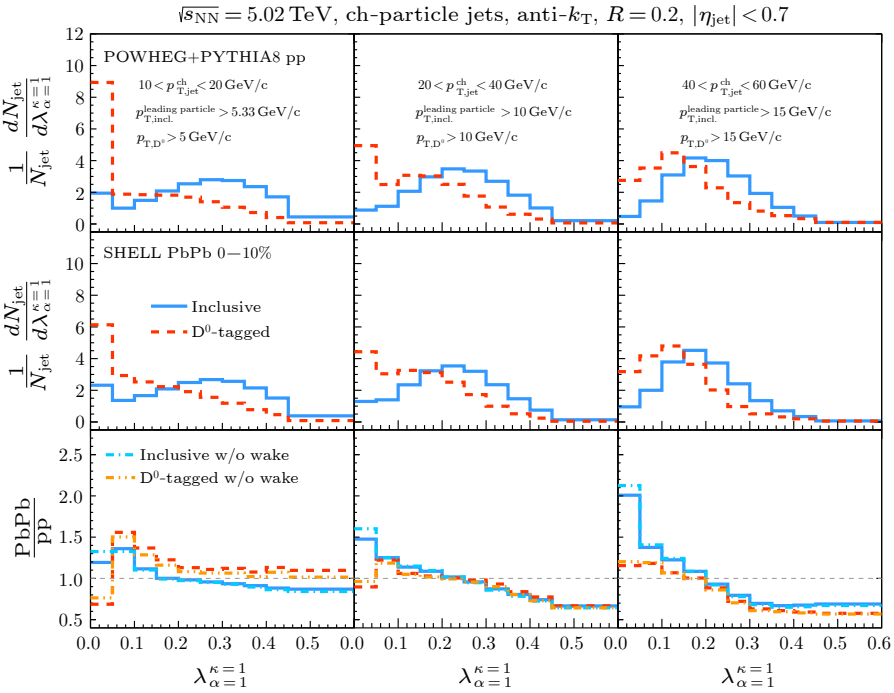

Fig. 4. Normalized angularity distributions of the $\rm D^0$-tagged and inclusive jets for three $p_{\rm T,jet}^{\rm ch}$ intervals: $10 < p_{\rm T,jet}^{\rm ch} < 20\,{\rm GeV/c}$, $20 < p_{\rm T,jet}^{\rm ch} < 40\,{\rm GeV/c}$ and $40 < p_{\rm T,jet}^{\rm ch} < 60\,{\rm GeV/c}$ (from left to right panels) in p+p (top panels) and 0–10% Pb+Pb (middle panels) collisions at $\sqrt{s_{\rm NN}} = 5.02$ TeV, as well as the ratios of Pb+Pb (with or without wake) over p+p (bottom panels).

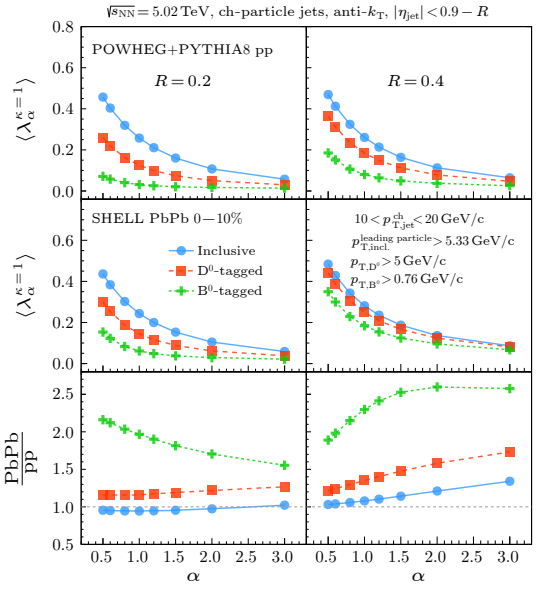

Fig. 5. Average angularities $\langle\lambda_\alpha^{\kappa=1}\rangle$ of inclusive, $\rm D^0$-tagged and $\rm B^0$-tagged jets within $10 < p_{\rm T,jet}^{\rm ch} < 20\,{\rm GeV/c}$ for two jet radii $R = 0.2$ (left panels) and $R = 0.4$ (right panels) in p+p (top panels) and 0–10% Pb+Pb (middle panels) collisions as a function of α, as well as the ratios of Pb+Pb over p+p (bottom panels).

Because the angularity values depend on both the momentum fraction and opening angle of the particles in the jets, it is of great interest to explore the mass dependence of the angularity modification with respect to the two corresponding parameters κ and α for inclusive and heavy-flavor jets. Hence, we also included the calculations of the average angularities for $\rm B^0$-tagged jets that mainly originate from the bottom quarks. In Fig. 5, we show average angularity values $\langle\lambda_\alpha^\kappa\rangle$ of inclusive, $\rm D^0$-tagged and $\rm B^0$-tagged jets as a function of the parameter α for $R = 0.2$ and $R = 0.4$ in p+p and 0–10% Pb+Pb collisions at $\sqrt{s_{\rm NN}} = 5.02$ TeV, as well as the ratios of PbPb/pp. In p+p collisions, $\langle\lambda_\alpha^\kappa\rangle$ decreases with quark mass. This is because heavier quarks suffer from a stronger influence of the "dead-cone" effect, with less gluon radiation during parton showers leading to smaller angularities. In Pb+Pb collisions, the ordering of $\langle\lambda_\alpha^\kappa\rangle$ values for the inclusive, $\rm D^0$-tagged, and $\rm B^0$-tagged jets was the same as that in pp. However, we observe that the ratios of PbPb/pp have a reversed ordering; that is, $\rm B^0$-tagged jets have the largest ratio, while inclusive jets have the smallest ratio. Because $\rm B^0$-tagged jets have smaller initial $\langle\lambda_\alpha^\kappa\rangle$ values, they are more sensitive to jet-medium interactions, such as $p_{\rm T}$ broadening and medium-induced gluon radiation, which

leads to broader jet angularities. For the larger jet radius $R = 0.4$ shown in the right panels, because more wide-angle particles from the medium-induced radiation and the medium response are included, one can see that the angularity broadening of heavy-flavor jets gets more significant compared to $R = 0.2$. In Fig. 6, we also tested the sensitivity of the jet angularity modifications to the parameter κ. Similarly, we obtained the same order of modification strength of the angularities (PbPb/pp) for the inclusive and heavy-flavor jets in the Pb+Pb collisions. However, because κ controls the weight of the particle momentum fraction, higher κ values suppress the contribution of the soft particles to the jets. Therefore, the ratios of PbPb/pp decrease with κ for all the jet types.

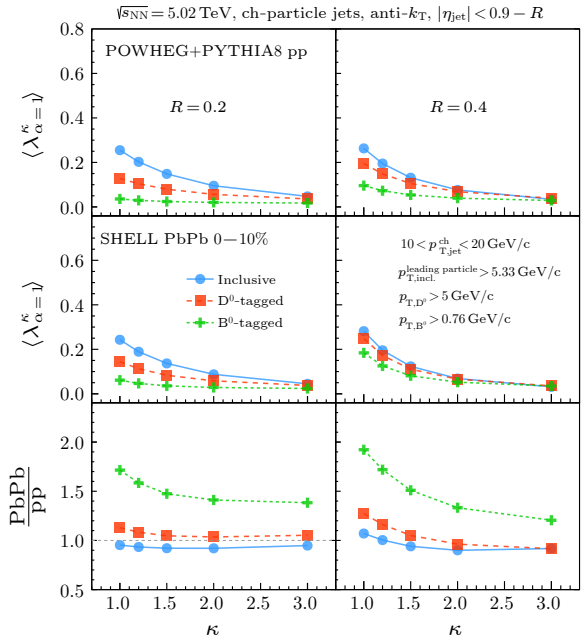

Fig. 6. Average angularities $\langle \lambda_\alpha^{\kappa=1} \rangle$ of inclusive, D^0-tagged and B^0-tagged jets within $10 < p_{\rm T,jet}^{\rm ch} < 20\,{\rm GeV/c}$ for two jet radii $R = 0.2$ (left panels) and $R = 0.4$ (right panels) in p+p (top panels) and 0–10% Pb+Pb (middle panels) collisions as a function of κ, as well as the ratios of Pb+Pb over p+p (bottom panels).

5. Summary. We present the first theoretical study on heavy-flavor jet angularities in Pb+Pb collisions at $\sqrt{s_{\rm NN}} = 5.02\,{\rm TeV}$. We used POWHEG+PYTHIA8 to simulate the initial heavy-flavor jet production in p+p collisions and employed the SHELL transport model to simulate the jet-medium interactions in nucleus-nucleus collisions. In p+p collisions, our calculated angularity distributions of the D^0-tagged jets are narrower than those of the inclusive jets, consistent with the preliminary ALICE data. This is because the inclusive jets contain a considerable fraction of gluon jets, which have broader angularity distributions than quark jets, whereas charm quarks primarily initiate the D^0-tagged jets. Additionally, the "dead-cone" effect suppresses gluon radiation at small angles for heavy quarks, resulting in a narrower angularity distribution compared to light-quark jets. In Pb+Pb collisions at $\sqrt{s_{\rm NN}} = 5.02\,{\rm TeV}$, our calculations show that jet-medium interactions in the QGP widen the angularity distributions of $R = 0.2$ D^0-tagged jets compared to the p+p baseline at $10 < p_{\rm T,jet}^{\rm ch} < 20\,{\rm GeV/c}$. Furthermore, the angularity distributions of the D^0-tagged and inclusive jets for $R = 0.2$ become narrower in Pb+Pb collisions than in p+p collisions at $p_{\rm T,jet}^{\rm ch} > 20\,{\rm GeV/c}$, where the influence of selection bias becomes significant, which is consistent with previous measurements at the LHC. By comparing the average angularity values $\langle \lambda_\alpha^\kappa \rangle$ of the inclusive D^0-tagged and B^0-tagged jets with varying α and κ, it can be observed that the larger the quark mass, the narrower the jet angularities. Because of the narrower initial distribution, we predict that heavy-flavor jets, especially the B^0-tagged jets, will experience stronger modifications of $\langle \lambda_\alpha^\kappa \rangle$ in Pb+Pb relative to the p+p baseline compared to inclusive jets. In addition, a more significant broadening of the jet angularities was observed for larger jet radii because of the enhanced contribution of wide-angle particles. Testing the predicted angularity broadening of heavy-flavor jets at low $p_{\rm T}$ and for large radii with an improved detector capability and increased luminosity at the LHC would be informative.

Acknowledgment. This research was supported by the Guangdong Major Project of Basic and Applied Basic Research (Grant No. 2020B0301030008) and the National Natural Science Foundation of China (Grant Nos. 11935007 and 12035007). S. W. was supported by the Open Foundation of the Key Laboratory of Quark and Lepton Physics (MOE) (Grant No. QLPL2023P01) and the Talent Scientific Star-up Foundation of the China Three Gorges University (CTGU) (Grant No. 2024RCKJ013).

References

[1] Freedman B A and McLerran L D 1977 *Phys. Rev. D* **16** 1169
[2] Shuryak E V 1978 *Sov. Phys. JETP* **47** 212
[3] Wang X N and Gyulassy M 1992 *Phys. Rev. Lett.* **68** 1480
[4] Gyulassy M, Vitev I, Wang X N, and Zhang B W 2003 arXiv:nucl-th/0302077 [nucl-th]
[5] Wang E and Wang X N 2002 *Phys. Rev. Lett.* **89** 162301
[6] Vitev I and Zhang B W 2010 *Phys. Rev. Lett.* **104** 132001
[7] Neufeld R B, Vitev I, and Zhang B W 2011 *Phys. Rev. C* **83** 034902
[8] Vitev I, Wicks S, and Zhang B W 2008 *J. High Energy Phys.* **2008(11)** 093
[9] He Y, Pang L G, and Wang X N 2020 *Phys. Rev. Lett.* **125** 122301
[10] Chen S Y, Yan J, Dai W, Zhang B W, and Wang E 2022 *Chin. Phys. C* **46** 104102
[11] Zhao W, Ke W, Chen W, Luo T, and Wang X N 2022 *Phys. Rev. Lett.* **128** 022302
[12] Yang Z, Luo T, Chen W, Pang L G, and Wang X N 2023 *Phys. Rev. Lett.* **130** 052301
[13] Yang Z, He Y, Moult I, and Wang X N 2024 *Phys. Rev. Lett.* **132** 011901
[14] Zhang H X, Xiao Y X, Kang J W, and Zhang B W 2022 *Nucl. Sci. Tech.* **33** 150
[15] Xie M, Han Q F, Wang E K, Zhang B W, and Zhang H Z 2024 *Nucl. Sci. Tech.* **35** 125

[16] Kumar A, Tachibana Y, Sirimanna C *et al.* [JETSCAPE] 2023 *Phys. Rev. C* **107** 034911
[17] Luo T, He Y, Cao S, and Wang X N 2024 *Phys. Rev. C* **109** 034919
[18] Zhang S L, Wang E, Xing H, and Zhang B W 2024 *Phys. Lett. B* **850** 138549
[19] Chen S Y, Shen K M, Dai W, Zhang B W, and Wang E K 2024 arXiv:2409.13996 [nucl-th]
[20] Xu J, Liao J, and Gyulassy M 2015 *Chin. Phys. Lett.* **32** 092501
[21] Ma Y G, Pang L G, Wang R, and Zhou K 2023 *Chin. Phys. Lett.* **40** 122101
[22] Wu J, Cao S, and Li F 2024 *Chin. Phys. Lett.* **41** 031202
[23] Yan J, Chen S Y, Dai W, Zhang B W, and Wang E K 2021 *Chin. Phys. C* **45** 024102
[24] Dong X and Greco V 2019 *Prog. Part. Nucl. Phys.* **104** 97
[25] Tang Z, Tang Z B, Zha W, Zha W M, Zhang Y, and Zhang Y F 2020 *Nucl. Sci. Tech.* **31** 81
[26] Wang S, Dai W, Wang E, Wang X N, and Zhang B W 2023 *Symmetry* **15** 727
[27] Zhao J, Zhou K, Chen S, and Zhuang P 2020 *Prog. Part. Nucl. Phys.* **114** 103801
[28] Francis A, Kaczmarek O, Laine M, Neuhaus T, and Ohno H 2015 *Phys. Rev. D* **92** 116003
[29] Kumar A, Majumder A, and Weber J H 2022 *Phys. Rev. D* **106** 034505
[30] Fan W, Vujanovic G, Bass S A *et al.* [JETSCAPE] 2023 *Phys. Rev. C* **107** 054901
[31] Xu Y, Bernhard J E, Bass S A, Nahrgang M, and Cao S 2018 *Phys. Rev. C* **97** 014907
[32] Li S and Liao J 2020 *Eur. Phys. J. C* **80** 671
[33] Cao S S, Coci G, Das S K *et al.* 2019 *Phys. Rev. C* **99** 054907
[34] Sirunyan A M, Tumasyan A, Adam W *et al.* [CMS] 2018 *Phys. Lett. B* **782** 474
[35] Adare A, Afanasiev S, Aidala C *et al.* [PHENIX] 2011 *Phys. Rev. C* **84** 054912
[36] Adamczyk L, Adkins J K, Agakishiev G *et al.* [STAR] 2014 *Phys. Rev. C* **90** 024906
[37] Abelev B, Adam J, Adamová D *et al.* [ALICE] 2014 *Phys. Lett. B* **738** 361
[38] Adamczyk L, Adkins J K, Agakishiev G *et al.* [STAR Collaboration] 2017 *Phys. Rev. Lett.* **118** 212301
[39] Sirunyan A M, Tumasyan A, Adam W *et al.* [CMS Collaboration] 2018 *Phys. Rev. Lett.* **120** 202301
[40] Adam J, Adamczyk L, Adams J R *et al.* [STAR] 2019 *Phys. Rev. Lett.* **123** 162301
[41] Adam J, Adamczyk L, Adams J R *et al.* [STAR] 2020 *Phys. Rev. Lett.* **124** 172301
[42] Vermunt L [ALICE] 2020 *PoS EPS-HEP* **364** 297
[43] Cacciari M, Nason P, and Vogt R 2005 *Phys. Rev. Lett.* **95** 122001
[44] Kniehl B A, Kramer G, Schienbein I, and Spiesberger H 2005 *Phys. Rev. D* **71** 014018
[45] Eskola K J, Paukkunen H, and Salgado C A 2009 *J. High Energy Phys.* **2009(04)** 065
[46] Eskola K J, Paakkinen P, Paukkunen H, and Salgado C A 2017 *Eur. Phys. J. C* **77** 163
[47] Cao S, Luo T, Qin G Y, and Wang X N 2016 *Phys. Rev. C* **94** 014909
[48] Li S, Xiong W, and Wan R 2020 *Eur. Phys. J. C* **80** 1113
[49] Xing W J, Cao S, and Qin G Y 2024 *Phys. Lett. B* **850** 138523
[50] Cao S, Sun K J, Li S Q, Liu S Y F, Xing W J, Qin G Y, and Ko C M 2020 *Phys. Lett. B* **807** 135561
[51] Plumari S, Minissale V, Das S K, Coci G, and Greco V 2018 *Eur. Phys. J. C* **78** 348
[52] He M and Rapp R 2020 *Phys. Rev. Lett.* **124** 042301
[53] Li H T and Vitev I 2019 *J. High Energ. Phys.* **2019** 148
[54] Kang Z B, Reiten J, Vitev I, and Yoon B 2019 *Phys. Rev. D* **99** 034006
[55] Dai W, Wang S, Zhang S L, Zhang B W, and Wang E 2020 *Chin. Phys. C* **44** 104105
[56] Li Y, Shen S W, Wang S, and Zhang B W 2024 *Nucl. Sci. Tech.* **35** 113
[57] Wang S, Dai W, Zhang B W, and Wang E 2023 *Chin. Phys. C* **47** 054102
[58] Wang S, Dai W, Zhang B W, and Wang E 2019 *Eur. Phys. J. C* **79** 789
[59] Wang S, Dai W, Zhang B W, and Wang E 2021 *Chin. Phys. C* **45** 064105
[60] Li Y, Wang S, and Zhang B W 2023 *Phys. Rev. C* **108** 024905
[61] Li H T and Vitev I 2019 *Phys. Lett. B* **793** 259
[62] Ringer F, Xiao B W and Yuan F 2020 *Phys. Lett. B* **808** 135634
[63] Tachibana Y, Kumar A, Majumder A *et al.* [JETSCAPE] 2023 arXiv:2301.02485 [hepph]
[64] Milhano G, Wiedemann U A, and Zapp K C 2018 *Phys. Lett. B* **779** 409
[65] Caucal P, Iancu E, and Soyez G 2019 *J. High Energ. Phys.* **2019** 273
[66] Wang L, Kang J W, Zhang Q, Shen S, Dai W, Zhang B W, and Wang E 2023 *Chin. Phys. Lett.* **40** 032101
[67] Acharya S, Adamová D, Adler A *et al.* [ALICE] 2023 *Phys. Rev. Lett.* **131** 192301
[68] Larkoski A J, Thaler J, and Waalewijn W J 2014 *J. High Energ. Phys.* **11** 129
[69] Dhankher P [ALICE] 2024 *PoS HardProbes* **2023** 140
[70] Caletti S, Fedkevych O, Marzani S, Reichelt D, Schumann S, Soyez G, and Theeuwes V 2021 *J. High Energ. Phys.* **07** 076
[71] Acharya S, Adamová D, Adler A *et al.* [ALICE] 2022 *JHEP* **05** 061
[72] Reichelt D, Caletti S, Fedkevych O, Marzani S, Schumann S, and Soyez G 2022 *JHEP* **03** 131
[73] Budhraja A, Sharma R, and Singh B 2023 arXiv:2305.10237 [hep-ph]
[74] Chien Y T, Fedkevych O, Reichelt D, and Schumann S 2024 *J. High Energ. Phys.* **07** 230
[75] Frixione S, Nason P, and Oleari C 2007 *JHEP* **11** 070
[76] Alioli S, Nason P, Oleari C, and Re E 2010 *J. High Energ. Phys.* **06** 043
[77] Bierlich C, Chakraborty S, Desai N, Gellersen L, Helenius I, Ilten P, Lönnblad L, Mrenna S, Prestel S, and Preuss C T *et al.* 2022 arXiv:2203.11601 [hep-ph]
[78] Alioli S, Hamilton K, Nason P, Oleari C and Re E 2011 *J. High Energ. Phys.* **04** 081
[79] Hou T J, Xie K, Gao J, Dulat S, Guzzi M, Hobbs T J, Huston J, adolsky P, Pumplin J, and Schmidt C *et al.* 2019 arXiv:1908.11394 [hep-ph]
[80] Cacciari M, Salam G P, and Soyez G 2012 *Eur. Phys. J. C* **72** 1896
[81] Caola F, Grabarczyk R, Hutt M L *et al.* 2023 *Phys. Rev. D* **108** 094010
[82] Banfi A, Salam G P, and Zanderighi G 2007 *JHEP* **07** 026
[83] Wang S, Li S, Li Y, Zhang B W, and Wang E 2024 arXiv:2410.21834 [hep-ph]
[84] Dokshitzer Y L and Kharzeev D E 2001 *Phys. Lett. B* **519** 199
[85] Acharya S *et al.* [ALICE] 2020 *Phys. Lett. B* **804** 135377
[86] Miller M L, Reygers K, Sanders S J, and Steinberg P 2007 *Ann. Rev. Nucl. Part. Sci.* **57** 205
[87] Acharya S, Acosta F T, Adamová D *et al.* [ALICE] 2018 *J. High Energ. Phys.* **10** 174
[88] Guo X F and Wang X N 2000 *Phys. Rev. Lett.* **85** 3591
[89] Zhang B W and Wang X N 2003 *Nucl. Phys. A* **720** 429

[90] Zhang B W, Wang E, and Wang X N 2004 *Phys. Rev. Lett.* **93** 072301
[91] Majumder A 2012 *Phys. Rev. D* **85** 014023
[92] Wang X N, Gyulassy M, and Plumer M 1995 *Phys. Rev. D* **51** 3436
[93] Zakharov B G 1996 *JETP Lett.* **63** 952
[94] Chen X F, Greiner C, Wang E, Wang X N, and Xu Z 2010 *Phys. Rev. C* **81** 064908
[95] Ma G Y, Dai W, Zhang B W, and Wang E K 2019 *Eur. Phys. J. C* **79** 518
[96] Pang L G, Petersen H, Wang Q, and Wang X N 2016 *Phys. Rev. Lett.* **117** 192301
[97] Pang L G, Petersen H, and Wang X N 2018 *Phys. Rev. C* **97** 064918
[98] Putschke J H, Kauder K, Khalaj E, Angerami A, Bass S A, Cao S, Coleman J, Cunqueiro L, Dai T, and Du L *et al.* 2019 arXiv:1903.07706 [nucl-th]
[99] Andersson B, Gustafson G, and Söderberg B 1983 *Z. Phys. C* **20** 317
[100] Chesler P M and Yaffe L G 2007 *Phys. Rev. Lett.* **99** 152001
[101] Casalderrey-Solana J, Gulhan D C, Milhano J G, Pablos D, and Rajagopal K 2017 *J. High Energ. Phys.* **03** 135
[102] Cooper F and Frye G 1974 *Phys. Rev. D* **10** 186
[103] Wang S, Li Y, Shen S, Zhang B W, and Wang E 2023 arXiv:2308.14538 [hep-ph]
[104] Aad G, Abbott B, Abbott D C *et al.* [ATLAS] 2023 *Eur. Phys. J. C* **83** 438
[105] Wang S, Kang J W, Dai W, Zhang B W, and Wang E 2022 *Eur. Phys. J. A* **58** 135
[106] Sirunyan A M, Tumasyan A, Adam W *et al.* [CMS] 2020 *Phys. Rev. Lett.* **125** 102001
[107] Vertesi R [ATLAS, CMS, and ALICE] 2024 arXiv:2405.16955 [nucl-ex]
[108] Larkoski A J, Marzani S, Soyez G, and Thaler J 2014 *J. High Energ. Phys.* **05** 146
[109] Renk T 2013 *Phys. Rev. C* **88** 054902
[110] Brewer J, Brodsky Q, and Rajagopal K 2022 *J. High Energ. Phys.* **02** 175
[111] Wang S, Li Y, Kang J W, and Zhang B W 2024 arXiv:2408.10924 [hep-ph]
[112] Kang J W, Wang S, Wang L, and Zhang B W 2023 arXiv:2312.15518 [hep-ph]